An Alternative Approach for Semi-Automatic Delineation of Rock Blocks on 3D Meshes and Engineering Application

Regine Tsui[1*], Jonathan Hart[2], Wenzhu Hou[2], Alan Ng[2]

[1]Aurecon Hong Kong Limited, Hong Kong, China
[2]GeoRisk Solutions Ltd., Hong Kong, China

*Corresponding author
doi: https://doi.org/10.21467/proceedings.133.14

ABSTRACT

Auto-identification of rock blocks on 3D models is a useful new tool for rock engineering. It has the potential, when undertaken with rock engineering professionals, to delineate remotely, potentially unstable rock blocks associated with adverse discontinuities. An alternative approach is proposed to semi-automatically delineate rock blocks on 3D meshes, which does not require prior extraction and fitting of discontinuity planes. The proposed approach starts with trace extraction, exploiting the fact that the contact between two rock blocks is most often manifested by a trace (i.e., an exposed line) on the rock surface. Geometrically, the trace is usually either a concave edge or a depressed line. These traces are first extracted due to their higher concavity or darkness compared to their neighbouring mesh faces. After post-processing, the mesh is segmented into sub-meshes around the extracted trace lines. The algorithms are implemented in Python and are tested on three rock slopes, including: (1) a rock slope in Ouray, USA; (2) a natural rock outcrop in Ma Shi Chau, Hong Kong; and (3) a rock slope in a former quarry currently being redeveloped as part of a large-scale site development in Hong Kong. Our approach can enrich the rock mapping results and help identify critical rock blocks which may be at risk of planar failure.

Keywords: Point Cloud, Rock Blocks, Discontinuity Traces

1 Introduction

In recent years, due to the increase in the capability of 3D data acquisition techniques, such as structure-from-motion (SfM) photogrammetry and laser scanning, accurate 3D models can be readily produced for rock surfaces. Auto-identification of rock blocks on 3D models is a useful new tool for rock engineering. It has the potential, when undertaken with rock engineering professionals, to delineate remotely, potentially unstable rock blocks associated with adverse discontinuities.

Compared with numerous research focused on discontinuity plane extraction and computation on 3D surface models (e.g., Vöge et al., 2013; Assali et al., 2014; Riquelme et al., 2014; Dewez et al., 2016; Kong et al., 2020; Zhang et al., 2018; Tsui et al., 2021), research centered on rock blocks on 3D surface models is at an early stage. Relevant research is largely motivated by attempts to estimate the block size, which is important in various rock mass classification schemes. For example, by statistical modelling, Mavrouli et al. (2015), Wichmann (2019), and Buyer et al. (2020) can estimate the rock block size distribution from characteristics of major discontinuity sets derived from the 3D models, either using equations or a stochastic discrete fracture network (DFN) generator. However, identification of the actual rock blocks from the 3D model is not required and is not a focus in the above research.

Chen et al. (2017) proposed a method that can extract regular, six-sided rock blocks formed by 3 discontinuity sets. Long et al. (2021) and Kong et al. (2021) further developed methods to detect rock blocks with more complex shapes (i.e. those formed by > 3 discontinuity sets), also by examining the intersection relationship of the discontinuities extracted. By considering discontinuity intersections, some of these methods are not only able to extract the exposed portions of the rock blocks, but also able

Proceedings DOI: 10.21467/proceedings.133; Series: AIJR Proceedings; ISSN: 2582-3922; ISBN: 978-81-957605-1-0

to reasonably predict the shape of the hidden portion of the rock blocks for volume calculation. However, these methods can only detect rock blocks wholly bounded by planar discontinuities. Under actual conditions, exposed rock blocks are frequently bounded by uneven, irregular surfaces on one or more sides, such as curved fractures formed by blasting, or portions of weathered rock. Whilst these surfaces may form part of the rock blocks, they may not be planar or persistent enough to be extracted automatically. This is particularly relevant in Hong Kong, where the granitic and volcanic rock slopes often contain extensive yet wavy and undulating sheeting joints.

Whilst an estimation of rock block volume is useful, if this is not part of the objective, it is unnecessary to predict hidden parts of the rock blocks. In this way, we propose an alternative approach to semi-automatically delineate rock blocks on 3D meshes, which does not require prior extraction and fitting of discontinuity planes. This is particularly applicable to irregular rock blocks not wholly bounded by planar discontinuities.

2 Approach and Assumptions

Since only the surface of the rock can be seen, the connectedness of the concealed portions of the rock blocks is uncertain. When geologists identify rock blocks on the rock surface, the identification is interpretive, with assumptions on the subsurface block contacts. Similarly, our semi-automatic block delineation approach is also interpretive and is based on the following two principal assumptions:

1. The contact between two adjacent exposed rock blocks will be exposed as a trace (i.e., an exposed line) on the rock surface. Geometrically, the trace is usually either a concave rock edge or a line of narrow opening. In terms of color, the line is often darker than its surroundings due to shadow. An example is shown in Figure 1.
2. Blocks are fully separated from adjacent rock blocks by the exposed traces on the rock surface.

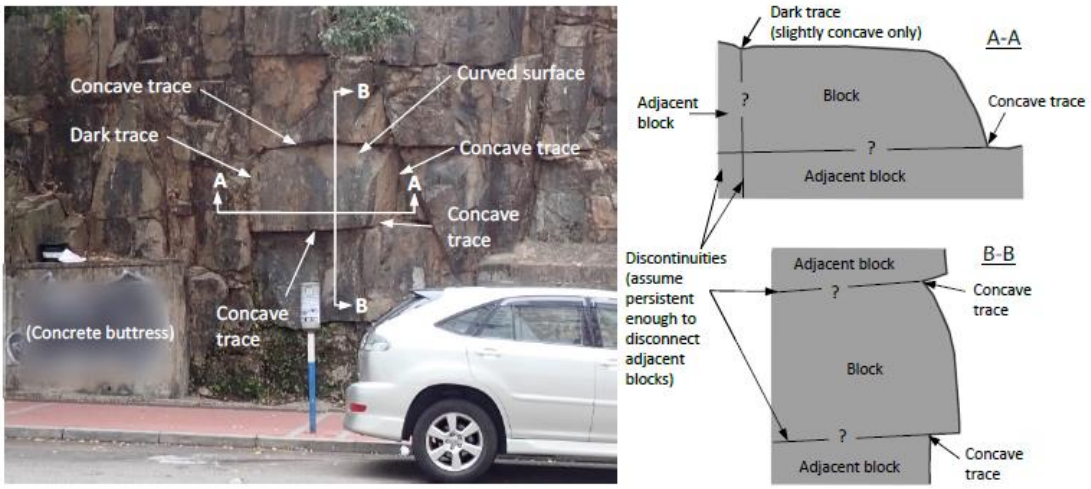

Figure 1: Example of a rock block with curved surfaces on a granite cut slope and the interpreted cross-sections. The contacts between the rock block and adjacent blocks are either concave edges or dark traces

The procedures of the proposed block delineation are summarized in Figure 2. Following assumption (1), the proposed approach starts by extracting traces, i.e. mesh faces representing concave rock edges or dark lines on the rock surface. These initial traces comprising the concave edges and the dark lines and are then combined. A threshold is set on the minimum number of faces contained by a connected trace group to reduce small, scattered noise. At this stage, some traces may not be extracted fully and are disconnected at place. In order to enhance the connection, dilation is then applied to the traces. In other words, a mesh face is recognized as part of the traces as long as any one of its closest *k* neighbors (where *k* is user-defined based on the resolution of the mesh) is classified as part of the traces. At the

Proceedings DOI: 10.21467/proceedings.133
ISBN: 978-81-957605-1-0

Series: AIJR Proceedings
ISSN: 2582-3922

end of this stage, the final traces form connected networks spanning most of the mesh to separate individual blocks.

In the next stage, the extracted traces are removed from the mesh. Individual rock blocks are then separated into isolated mesh components. Each isolated component of the mesh is then labelled as an individual rock block.

The initial result of the block delineation contains holes left by the traces. For noise reduction, a threshold is set on the minimum number of faces contained by the blocks to avoid tiny groups of mesh faces from being labelled as blocks. To restore the blocks' boundaries and to fill holes in the delineated mesh, mesh faces belonging to the traces or the discarded rock blocks are simply grouped into their closest labeled blocks.

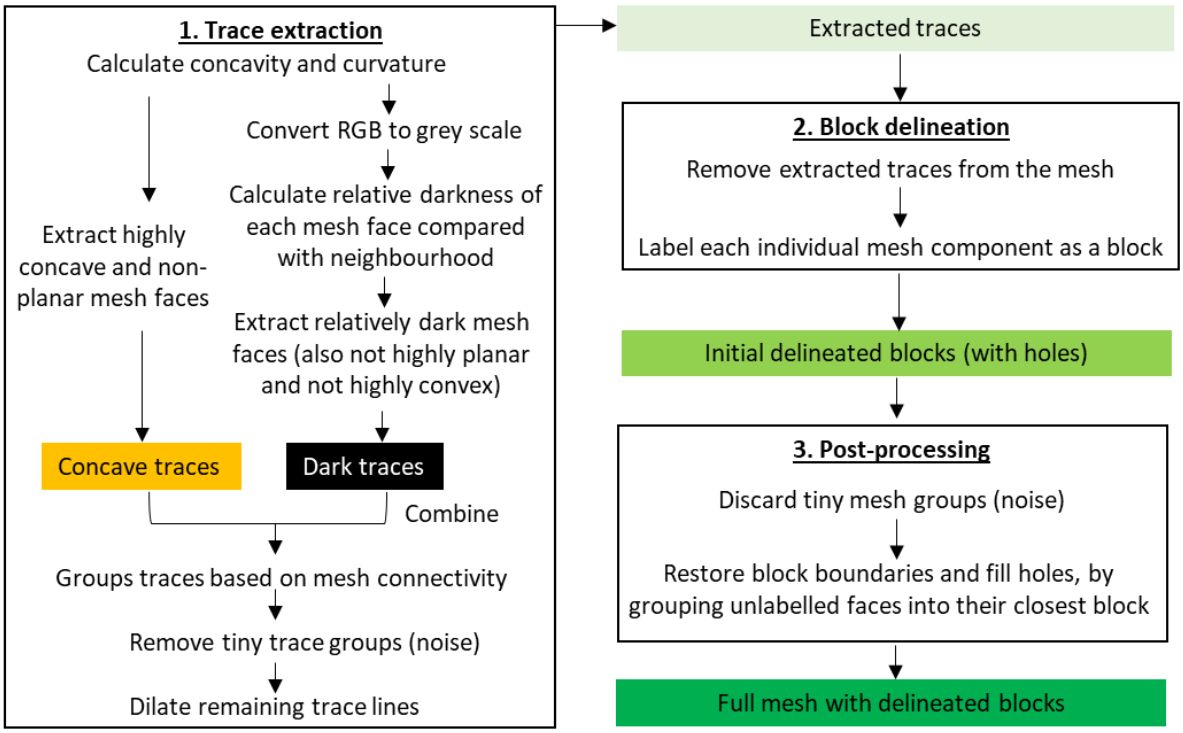

Figure 2: Procedures of block delineation

Our approach is implemented in Python scripts. The analysis relies heavily on the following widely used, well tested and free Python packages, as shown in Table 1:

Table 1: Python packages used in the analysis

Python packages	Usage
Trimesh (Dawson-Haggerty et al. 2019)	Mesh input / output, general mesh manipulations
NumPy (Harris et al. 2020)	Principal component analysis, and other operations on matrices
SciPy (Virtanen et al. 2020)	Finding connected components on meshes; k-nearest neighbor search

3 Application of Block Delineation

The most crucial part of our approach is trace extraction. Various semi-automatic trace extraction workflows have already been proposed for 3D surface models of rock mass, which operate on meshes (Umili et al. 2013, Li et al. 2016, Cao et al. 2017, Guo et al. 2019, Zhang et al. 2020), point clouds (Thiele et al. 2017, Guo et al. 2018), grid cells (Bolkas et al 2018), or a combination of point clouds and images (Zhang et al. 2019, Lee et al. 2022). Comprehensive reviews of most of the above trace extraction techniques can be found in Battulwal et al. (2020) and Umili (2021).

Most trace extraction methods are based on geometry (e.g., curvature) alone, while some are based on colours (i.e., RGB values) alone. Few (e.g., Guo et al. 2019) consider both geometry and colours at the same time. While most point clouds produced by SfM photogrammetry or terrestrial laser scanning are coloured nowadays, occasionally the RGB values are not available. Therefore, we tried two cases, one only extracts concave edges based on geometry, while the other also extracts dark lines by considering RGB values.

3.1 Block Delineation Based on Concave Trace

The point cloud data generated from terrestrial laser scanning of a quartzite rock slope in Ouray, Colorado, USA was selected as a trial. The point cloud was originally hosted in the Rockbench repository (Lato et al. 2013) and has been widely used in digital rock mass research (e.g., Riquelme et al. 2014, Li et al. 2016, Guo et al. 2018). The rock slope is approximately 20m long by 15m high. The retrieved point cloud was not colored. Meshing was performed in CloudCompare (CloudCompare 2017).

Figure 3: Roadside cut slope in Ouray, Colorado. Originally hosted in the Rockbench repository (Lato et al. 2013)

However, for block delineation purpose, we need to extract concave faces only. To extract concave mesh faces as traces, we estimated the concavity *c* of each face by

$$c = \left(\overline{\boldsymbol{f_k}} - \boldsymbol{f}\right) \cdot \boldsymbol{n} \quad \textbf{(1)}$$

Where $\boldsymbol{f}$ is the position vector ([x, y, z]) of the centroid of the mesh face, $\overline{\boldsymbol{f_k}}$ is the mean position of the centroids of the k-nearest neighbours of the face, and $\boldsymbol{n}$ is the unit vector along the direction normal to the mesh face.

The computed concavity on the mesh is shown in Figure 4 (Right). However, the results contain significant noise which is difficult to be differentiated from the true edges, mostly due to natural undulations which create concave spots and patches (i.e., irregularities) on the rock surface.

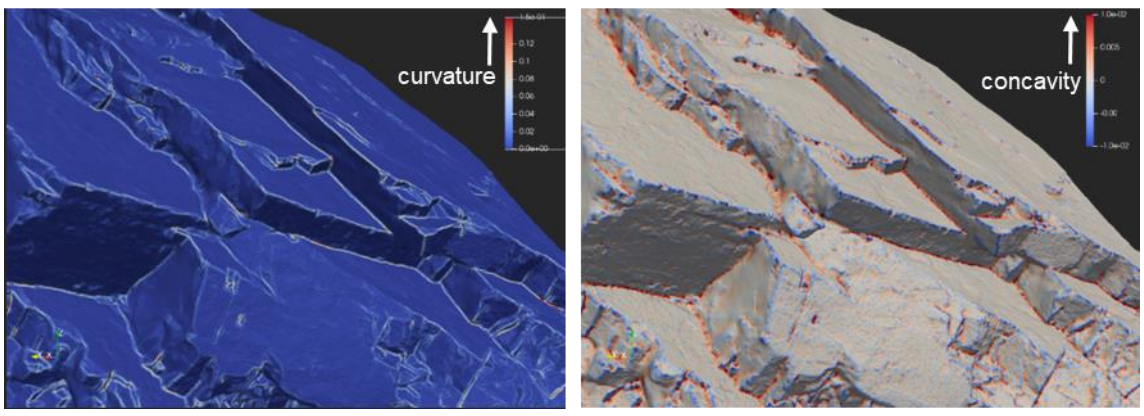

Figure 4: Calculated curvature (Left) and concavity (Right) values on the mesh

Proceedings DOI: 10.21467/proceedings.133
ISBN: 978-81-957605-1-0

Series: AIJR Proceedings
ISSN: 2582-3922

It is found that incorporating the curvature can improve the results, as the neighbourhood of the concave undulations are in fact generally planar. Due to ease of computation, the method used in Riquelme et al. (2014) and Wang et al. (2017) for checking planarity was used to estimate the curvature. To estimate the local curvature (σ) of a face, eigendecomposition is carried out on the covariance matrix of the centroids of its neighbouring faces. This gives three pairs of orthogonal eigenvectors and eigenvalues (λ_1, λ_2 and λ_3, where $\lambda_1 \geq \lambda_2 \geq \lambda_3$). Curvature σ can then be estimated by Pauli et al. (2002):

$$\sigma = \frac{\lambda_3}{\lambda_1 + \lambda_2 + \lambda_3} \quad \textbf{(2)}$$

The calculated curvature on the mesh is shown in Figure 4. Based on trial and error, mesh faces with the 30% highest concavity and the 40% highest curvature are extracted as concave traces. After refining the traces and delineating the blocks following procedures as discussed in Figure 2, the final traces and the block delineation results are shown in Figure 5.

The results show that the delineation is overall satisfactory and that the larger blocks, such as the three rock slabs on the crest of the slope, are extracted rather accurately. In the more fractured areas, e.g. close to the left toe of the rock slope, the block boundaries are less accurate.

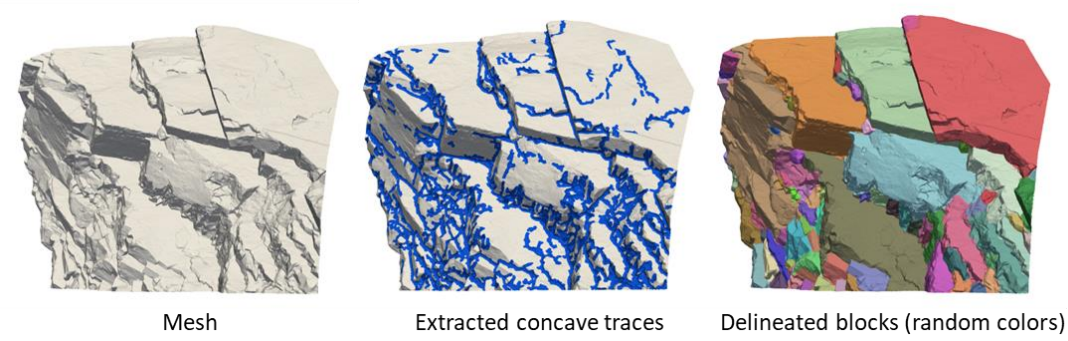

Figure 5: Results of block delineation on the rock cut in Ouray

3.2 Block Delineation Based on Concave Trace and Dark Trace

A rock outcrop in Ma Shi Chau, Hong Kong, is selected to test block delineation based on concave and dark traces. The rock outcrop is approximately 2m long and comprises sandstone from the Permian Tolo Harbour Formation. Since the outcrop is located along the coast, the surface is weathered and relatively rounded due to coastal erosion. The outcrop contains multiple sets of discontinuities which form networks of traces on the surface (Figure 6). The point cloud was generated by SfM photogrammetry from 24 photos using the software Agisoft Metashape Standard. The point cloud was scaled and orientated accurately based on reference objects in the field. Meshing was carried out in CloudCompare (CloudCompare, 2017).

Trace-extraction methods based on colours (Guo et al. 2018, Zhang et al. 2019, Lee et al. 2022) make use of sophisticated edge-detection algorithms on 2D images to extract the edges or dark lines and map the traces back to the 3D surface models. In this study, we just compute the relative darkness (i.e., opposite of brightness) of individual faces by comparing their brightness to the average brightness of their k-nearest neighbourhood directly, which appears to work well enough to recognize the dark traces (Figure 7). To simplify the calculation, the RGB values are first converted to grey-scale brightness by taking average of the RGB values. The equation for the relative darkness is simply as follows:

Relative Darkness = B_k / B **(3)**

Where B is the brightness of the mesh face and B_k is the average brightness of the k-nearest neighborhood of the mesh face.

In this study, traces with the 35% highest relative darkness are extracted, based on trial and error. Extraction of traces based on relative darkness are capable of extracting traces which are less concave compared to those extracted purely based on geometry, i.e. concavity and curvature (as shown in Figure 7).

However, since a few locally dark areas (such as weathering stains) are still extracted inaccurately as traces, we further add constraints based on the concavity and the curvature on the dark traces to filter faces with low concavity and curvature. Finally, these are combined with the extracted concave traces and are refined according to procedures in Figure 2. The final traces and the block delineation results are presented in Figure 6 and these are in overall good agreement with the visual interpretation. The results show that our approach can work on rock blocks bounded by weathered surfaces as well.

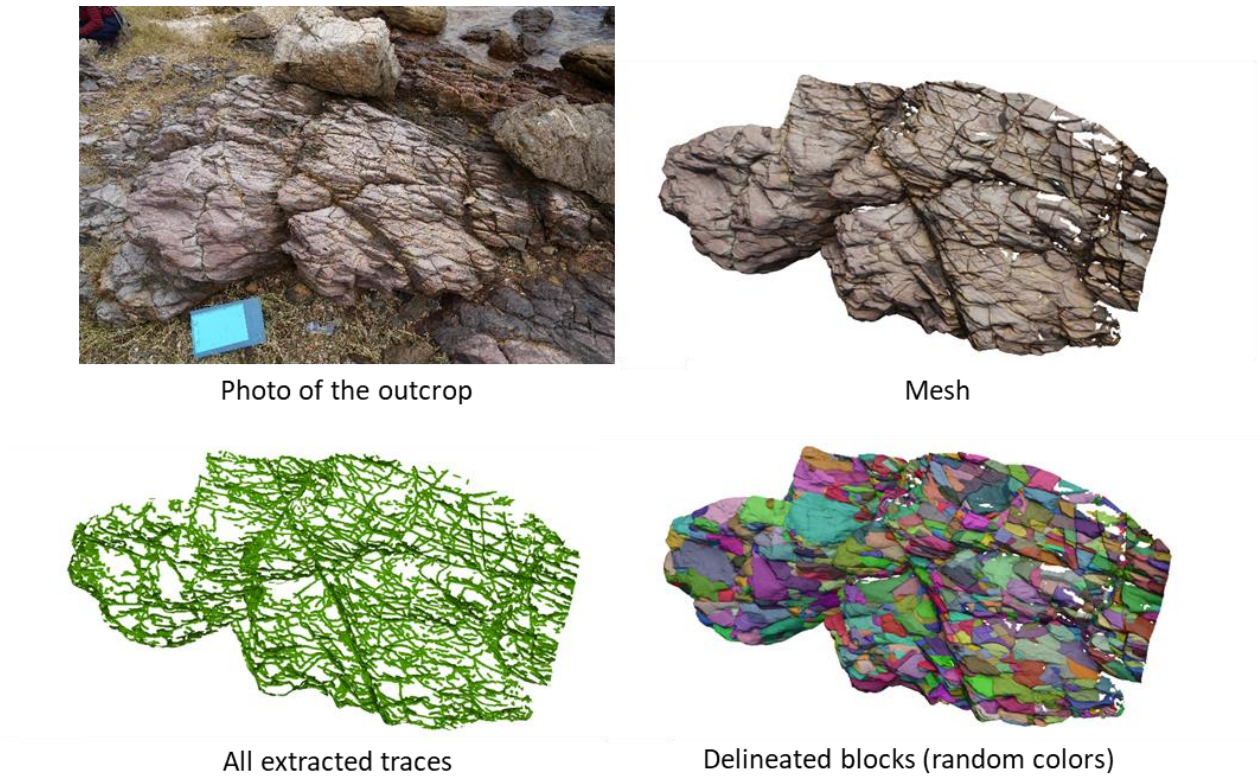

Figure 6: Block delineation of the rock outcrop in Ma Shi Chau

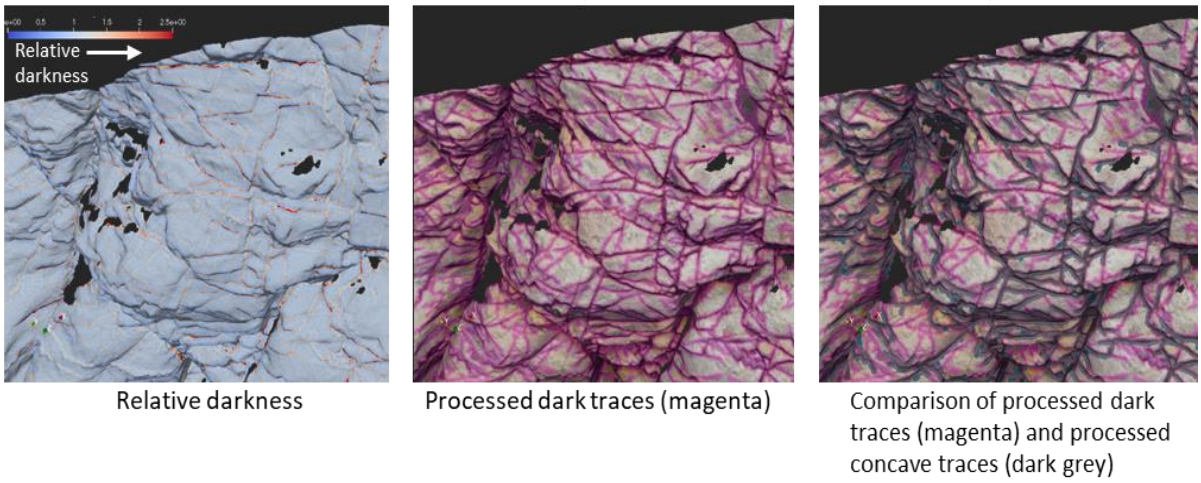

Figure 7: Extraction of traces based on relative darkness

Proceedings DOI: 10.21467/proceedings.133
ISBN: 978-81-957605-1-0

Series: AIJR Proceedings
ISSN: 2582-3922

4 Engineering Application – Potentially Unstable Blocks

A possible engineering application of block delineation is to delineate potentially unstable rock blocks. Previously we presented an approach to detect intersections which indicate potential planar sliding blocks in Tsui et al. (2021). The technique has the advantage of not requiring to assume a uniform slope orientation, compared to traditional kinematic analysis based on stereonets. In the case study provided below, we use the technique in conjunction with block delineation to give more relevant results.

This application is tested on an existing rock slope at a former quarry in Hong Kong. The rock slope was formed with a slope face dipping at 60° and predominantly comprises Grade II granite. The slope was surveyed by an unmanned aerial vehicle (UAV). A point cloud was constructed from the UAV photos by SfM photogrammetry using the software Agisoft Metashape Standard. Georeferencing was carried out with reference to ground control points. An area measuring approximately 15m long by 8m high, which does not contain vegetation and man-made structures, was selected for analysis (red box in Figure 8). The slope was also mapped manually on an elevated working platform.

Figure 8: Photo of the studied existing slope at a former quarry in Hong Kong. Red box: studied portion

Following the procedures in Figure 2, we extracted both concave traces and dark traces on the mesh (50% highest in concavity and 40% highest in curvature, with 10% highest in relative darkness) based on trial and error. The delineated blocks are shown in Figure 9. Overall, the results are consistent with our visual interpretation, except that the block boundaries are less accurate at the right toe of the slope where the rock is more heavily fractured.

Figure 9: Results of block delineation

Our intersection-based planar sliding detection approach works by checking whether concave edges exist above an extracted discontinuity, as this indicates that the discontinuity is "daylighting" and a block may be present on top of it. If a daylighting discontinuity dips steeper than the friction angle, the block may slide along its surface. Our first step is to extract the discontinuities on the slope by the approach used in Tsui et al. (2021). The results are shown in Figure 10. For demonstration purposes only, a low friction angle (25°) was adopted to search for any potentially adverse daylight-indicating intersections, such that more unstable blocks are yielded in the demonstration exercise.

Figure 10: Results of joint extraction and search for potentially adverse daylight-indicating intersections (yellow arrow: invalid intersection)

In the next stage, we check whether the daylight-indicating intersections are really located at the base of any blocks. This step is carried out because the search for daylight-indicating intersections often picks up rock undulations which have no apparent side release mechanism (e.g., yellow arrow in Figure 10). To some extent, by checking with the block delineation results, this step also takes into consideration the availability of side release surfaces.

The interpreted, potentially unstable blocks are shown in Figure 11. Overall, the results are similar to those from our mapping, although the mapping also identified areas with potential ravelling and rockfall mechanisms, which are not checked in this semi-automated approach. A few small blocks were also missed in the semi-automated approach, due to inaccurate discontinuity or block boundaries.

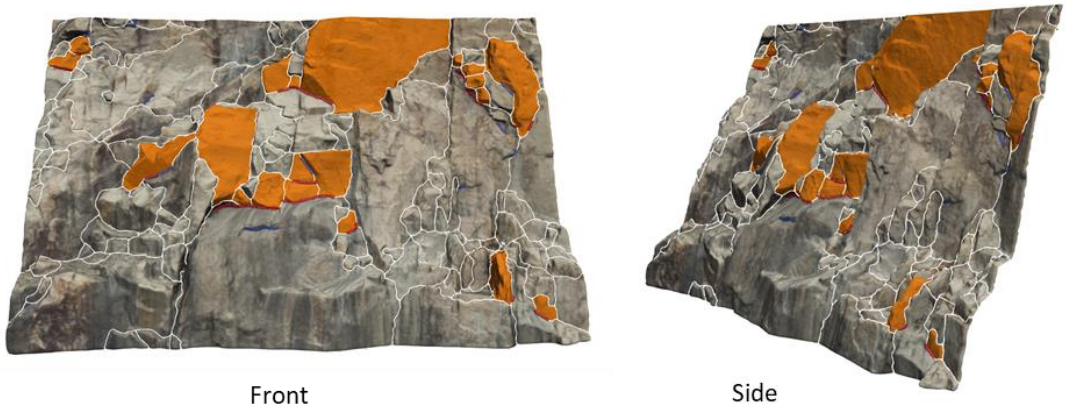

Figure 11: Highlighting potentially unstable blocks associated with adverse discontinuities

5 Discussions

5.1 Advantages

Our approach of block delineation has the following advantages:

1. It does not require prior discontinuity plane extraction and it is not affected by the performance of the plane extraction process. In addition, block detection techniques based on plane extraction may not be applicable when the exposed discontinuity planes are limited, for

Proceedings DOI: 10.21467/proceedings.133
ISBN: 978-81-957605-1-0

Series: AIJR Proceedings
ISSN: 2582-3922

example, the rock outcrop in Ma Shi Chau (Section 3.2). Extraction of traces is a more versatile solution in this situation.

2. Rock blocks not wholly bounded by planar discontinuities (e.g., partially bounded by weathered surfaces) can also be delineated. This is particularly relevant in Hong Kong where rock blocks may be located above irregular sheeting-like joints in weathered granite and volcanic rocks.
3. In rock slope mapping, it is not routine to interpret the block boundaries on the whole slope. Our approach provides a semi-automated way to do so, which may enhance the mapping results. In addition, delineating blocks on the rock slope can assist in rock mass characterization.
4. When linked with kinematic analysis, the results may help locate potentially unstable planar blocks for stabilization. A quick analysis can be carried out remotely as a preliminary safety check before direct rock slope mapping is undertaken. This is also an alternative solution when only remote (i.e. indirect) mapping can be carried out.
5. The entire block delineation process from trace extraction to post processing is very quick (completed under 3 minutes) on a computer with Intel Core i7-9750H and 32 GB RAM. For reference, the meshes in the case studies contain 1.9 million to 8.8 million faces, with surveyed areas ranging from approximately 3m^2 (for the rock outcrop) to 120m^3 and 300m^2 (for the rock slopes).

5.2 Limitations

1. This approach assumes that the contact between two adjacent exposed rock blocks will be exposed as a trace on the rock surface. However, extremely narrow joints (i.e. with small aperture) which appear as very thin dark lines and are not obviously concave may still be missed in the trace extraction. As a result, two blocks may be labelled as one.
2. This approach assumes that blocks are fully separated by exposed traces on the rock surface. However, in reality, the true subsurface persistence of these discontinuities is not known. In addition, these are also likely to contain rock bridges which still connect the adjacent blocks. Whether or not there are discontinuities 'hidden' at the back of the block to disconnect it from the overall rock mass, is also not known. Figure 12 illustrates the above uncertainties. Therefore, the delineation is a conservative interpretation.

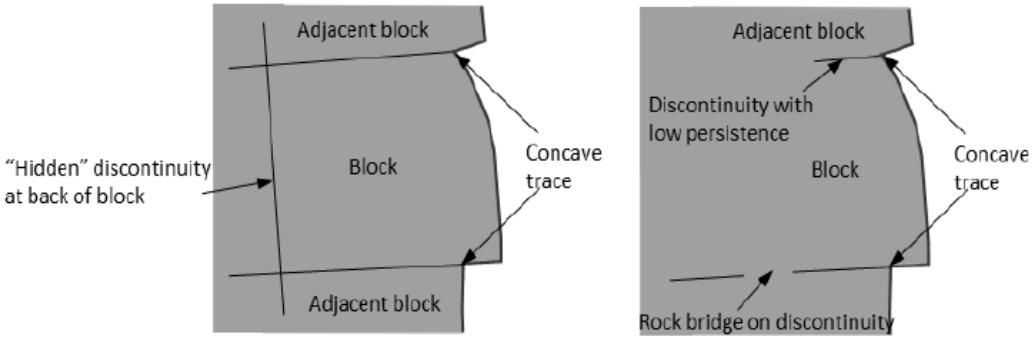

Figure 12: Schematic cross-sections showing two possible scenarios when a block is seemingly enclosed by concave traces on the surface. Left: The block is isolated. Right: The block is still connected with adjacent blocks.

3. The approach works for concave rock blocks (Figure 13, left). However, if the rock block contains areas enclosed by sharp concave edges, these areas may be misidentified as separate blocks (Figure 13, right). In addition, the approach does not perform well for highly fractured areas, as these areas are full of extracted traces that mask the blocks.

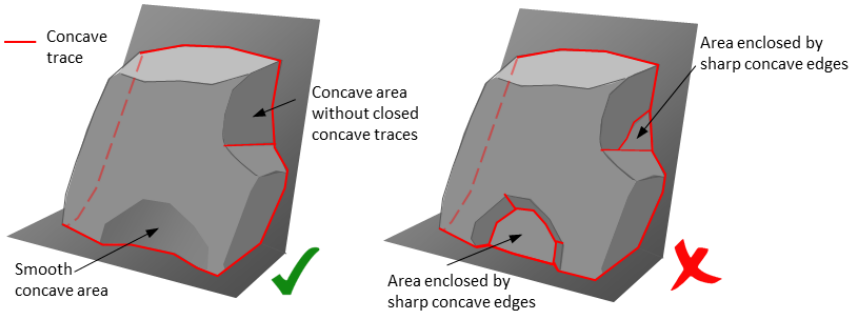

Figure 13: Example of a rock block with areas enclosed by sharp concave edges (Right) and one which does not (Left)

4. The approach relies on the user to set various thresholds to extract the traces and the post-processing steps. These thresholds need to be fine-tuned as these are specific for each site and depends on the resolution of the mesh.
5. In our last case study (Section 4), we only focused in planar sliding, which is just one mode of block failure mechanism. Other mechanisms, like toppling and wedge failures, are not considered at present, especially for small blocks or discontinuities of very low persistence. In addition, the discontinuity characteristics such as infilling, roughness, and alteration, are not taken into account.

5.3 Further investigations

Potential further investigations to improve the method include:

1. To carry out more case studies to find automatic ways to define the thresholds. Machine-learning approaches can be explored.
2. To modify the approach such that it can be applied on point clouds directly instead of meshes. Point clouds retain more information than meshes.
3. To estimate the volumes of the extracted blocks, for example, by using convex hull on the exposed portions of the rock blocks. Our current approach cannot directly calculate the block volume, as it does not predict hidden parts of the rock blocks.

6 Conclusions

This study proposes and describes an alternative, semi-automatic approach to delineate rock blocks on 3D meshes of rock surfaces based on traces. The proposed block delineation approach relies on the extraction of concave traces and dark traces based on curvature and colours respectively. An area on the mesh which is enclosed by concave or dark traces is then interpreted as a block. Our approach is demonstrated satisfactorily for three case studies involving a natural outcrop and two rock cut slopes, one of which is a mapped rock slope in Hong Kong. In one case study, we identified intersections associated with potential planar failure and linked these with the delineated blocks to highlight those blocks that are potentially unstable. Although these semi-automatic techniques cannot replace field verification by geologists, our approach can enhance the field mapping results, assist in locating areas which require stabilization and enhance the site safety.

7 Declarations

7.1 Acknowledgements

The point cloud data from the Ouray rock cut was retrieved from Dr. Riquelme's personal website (https://personal.ua.es/en/ariquelme/a-new-approach-for-semi-automatic-rock-mass-joints-recognition-

from-lidar-data.html). The dataset was formerly hosted on the Rockbench open repository (www.rockbench.org).

We would like to thank Miss Sonia Hui and others for their kind field assistance in Ma Shi Chau, and Mr Chison Cheung for part of the mapping work of the granite rock slope.

7.2 Publisher's Note

AIJR remains neutral with regard to jurisdictional claims in published maps and institutional affiliations.

References

Assali, P., Grussenmeyer, P., Villemin, T., Pollet, N. & Viguier, F. 2014. Surveying and modeling of rock discontinuities by terrestrial laser scanning and photogrammetry: Semi-automatic approaches for linear outcrop inspection. Journal of Structural Geology, 66, 102-114

Battulwar, R.; Zare-Naghadehi, M.; Emami, E. & Sattarvand, J. 2021. A state-of-the-art review of automated extraction of rock mass discontinuity characteristics using three-dimensional surface models. Journal of Rock Mechanics and Geotechnical Engineering, 13, 920-936

Bolkas, D.; Vazaios, I.; Peidou, A. & Vlachopoulos, N. 2018. Detection of Rock Discontinuity Traces Using Terrestrial LiDAR Data and Space-Frequency Transforms. Geotechnical and Geological Engineering, 36, 1745-1765

Buyer, A., Aichinger, S. & Schubert, W. 2020. Applying photogrammetry and semi-automated joint mapping for rock mass characterization. Engineering Geology, 264, 105332

Cao, T.; Xiao, A.; Wu, L. & Mao, L. Automatic fracture detection based on Terrestrial Laser Scanning data: A new method and case study. 2017. Computers & Geosciences, 106, 209-216

CloudCompare (version 2.9). 2017. Retrieved from http://www.cloudcompare.org/

Chen, N., Kemeny, J., Jiang, Q. & Pan, Z. 2017. Automatic extraction of blocks from 3D point clouds of fractured rock. Computers & Geosciences, 109, 149 – 161

Dawson-Haggerty et al. 2019. Trimesh (version 3.2.0). https://trimsh.org/

Dewez, T. J. B., Girardeau-Montaut, D., Allanic, C. & Rohmer, J. 2016. Facets: A CloudCompare Plugin To Extract Geological Planes From Unstructured 3d Point Clouds. Int. Arch. Photogramm. Remote Sens. Spatial Inf. Sci., XLI-B5, 799-804

Guo, J.; Wu, L.; Zhang, M.; Liu, S. & Sun, X. 2018. Towards automatic discontinuity trace extraction from rock mass point cloud without triangulation. International Journal of Rock Mechanics and Mining Sciences, 112, 226 - 237

Guo, J.; Liu, Y.; Wu, L.; Liu, S.; Yang, T.; Zhu, W. & Zhang, Z. 2019. A geometry- and texture-based automatic discontinuity trace extraction method for rock mass point cloud. International Journal of Rock Mechanics and Mining Sciences, 124, 104132

Kong, D., Wu, F. & Saroglou, C. 2020. Automatic identification and characterization of discontinuities in rock masses from 3D point clouds. Engineering Geology, 265, 105442

Kong, D., Wu, F., Saroglou, C., Sha, P. & Li, B. 2021. In-Situ Block Characterization of Jointed Rock Exposures Based on a 3D Point Cloud Model. Remote Sensing, 13

Lato, M., Kemeny, J., Harrap, R. & Bevan, G. 2013. Rock bench: Establishing a common repository and standards for assessing rockmass characteristics using LiDAR and photogrammetry. Computers & Geosciences, 50, 106 – 114

Lee, Y.-K.; Kim, J.; Choi, C.-S. & Song, J.-J. 2022. Semi-automatic calculation of joint trace length from digital images based on deep learning and data structuring techniques. International Journal of Rock Mechanics and Mining Sciences, 149, 104981

Li, X.; Chen, J. & Zhu, H. 2016. A new method for automated discontinuity trace mapping on rock mass 3D surface model. Computers & Geosciences, 89, 118-131

Long, Y., Huang, Q., Wu, F., Yi, H., Guan, S. & Sha, P. 2021. Automatic identification of irregular rock blocks from 3D point cloud data of rock surface. IOP Conference Series: Earth and Environmental Science, IOP Publishing, 861, 022048

Mavrouli, O., Corominas, J. & Jaboyedoff, M. 2015. Size Distribution for Potentially Unstable Rock Masses and In Situ Rock Blocks Using LIDAR-Generated Digital Elevation Models. Rock Mechanics and Rock Engineering, 48, 1589-1604

Pauly, M., Gross, M., & Kobbelt, L. P. 2002. Efficient simplification of point-sampled surfaces. In IEEE Visualization, October 2002. VIS 2002. IEEE.

Riquelme, A. J., Abellán, A., Tomás, R. & Jaboyedoff, M. 2014. A new approach for semi-automatic rock mass joints recognition from 3D point clouds. Computers & Geosciences, 68, 38-52

Thiele, S. T.; Grose, L.; Samsu, A.; Micklethwaite, S.; Vollgger, S. A. & Cruden, A. R. 2017. Rapid, semi-automatic fracture and contact mapping for point clouds, images and geophysical data. Solid Earth, 8, 1241-1253

Tsui, R., Cheung, C., Hart, J., Hou, W. & Ng, A. 2021. Intersection-based potential plane failure detection on 3D meshes for rock slopes. In Proceedings of the HKIE Geotechnical Division 41st Annual Seminar, pp. 256-268.

Virtanen, P., Gommers, R., Oliphant, T.E., Haberland, M., Reddy, T., Cournapeau, D., . . .SciPy 1.0 Contributors. 2020. SciPy 1.0: Fundamental Algorithms for Scientific Computing in Python. Nature Methods, 17, 261–272.

Vöge, M., Lato, M. J. & Diederichs, M. S. 2013. Automated rockmass discontinuity mapping from 3-dimensional surface data. Engineering Geology, 164, 155-162

Wang, X.; Zou, L.; Shen, X.; Ren, Y. & Qin, Y. 2017. A region-growing approach for automatic outcrop fracture extraction from a three-dimensional point cloud. Computers & Geosciences, 99, 100 - 106

Wichmann, V., Strauhal, T., Fey, C. & Perzlmaier, S. 2019. Derivation of space-resolved normal joint spacing and in situ block size distribution data from terrestrial LIDAR point clouds in a rugged Alpine relief (Kühtai, Austria). Bulletin of Engineering Geology and the Environment, 78, 4465-4478

Umili, G.; Ferrero, A. & Einstein, H. H. A new method for automatic discontinuity traces sampling on rock mass 3D model. 2013. Computers & Geosciences, 51, 182-192.

Umili, G. Methods for sampling discontinuity traces on rock mass 3D models: state of the art. IOP Conference Series: Earth and Environmental Science, IOP Publishing, 2021, 833, 012050

Zhang, P., Du, K., Tannant, D. D., Zhu, H. & Zheng, W. 2018. Automated method for extracting and analysing the rock discontinuities from point clouds based on digital surface model of rock mass. Engineering Geology, 239, 109 – 118.

Zhang, P.; Zhao, Q.; Tannant, D. D.; Ji, T. & Zhu, H. 2019. 3D mapping of discontinuity traces using fusion of point cloud and image data. Bulletin of Engineering Geology and the Environment, 78, 2789-2801

Zhang, K.; Wu, W.; Zhu, H.; Zhang, L.; Li, X. & Zhang, H. 2020. A modified method of discontinuity trace mapping using three-dimensional point clouds of rock mass surfaces. Journal of Rock Mechanics and Geotechnical Engineering, 12, 571 - 586